DALTON

Synthesis and characterisation of three Group 10 metal dithiadiazolyl complexes‡

Arthur J. Banister,[a] Ian B. Gorrell,[a] Judith A. K. Howard,[a] Simon E. Lawrence,[a] Christian W. Lehman,[a] Iain May,[a] Jeremy M. Rawson,*†[a] Brian K. Tanner,[b] Christopher I. Gregory,[b] Alexander J. Blake†[c] and Simon P. Fricker[d]

[a] *Department of Chemistry, The University of Durham, South Road, Durham DH1 3LE, UK*
[b] *Department of Physics, The University of Durham, South Road, Durham DH1 3LE, UK*
[c] *Department of Chemistry, The University of Edinburgh, West Mains Road, Edinburgh EH9 3JJ, UK*
[d] *Johnson-Matthey Technology Centre, Blount's Court, Sonning Common, Reading RG4 9NH, UK*

Reaction of $(PhC\overline{NSSN})_2$ with $[Pt(PPh_3)_3]$ or $[Pt(PPh_3)_4]$ produced two complexes $[Pt\{SNC(Ph)NS\text{-}S,S'\}(PPh_3)_2]$ **1** and $[Pt_3\{\mu\text{-}SNC(Ph)NS\text{-}S,S'\}_2(PPh_3)_4]$ **2**. In contrast, reaction with $[Pd(PPh_3)_4]$ yielded only the trimetallic complex $[Pd_3\{\mu\text{-}SNC(Ph)NS\text{-}S,S'\}_2(PPh_3)_4]$ **3**. The three complexes were characterised by X-ray crystallography as the following solvates: **1**·MeCN, **2**·$2C_6H_5Me$ and **3**·$2CH_2Cl_2$. In all three structures the S–S bond is formally broken [d_{ss} in **1**, **2** and **3** are 3.168(4), 3.046(8) and 3.044(8) Å respectively], the metals increase their oxidation states to +2 and possess square-planar co-ordination geometries. The physical properties of the complexes are described and the biological activities of **1** and **2** are reported.

We recently outlined[1] the syntheses and solid-state structures of two dithiadiazolyl complexes of platinum, $[Pt\{SNC(Ph)NS\text{-}S,S'\}(PPh_3)_2]$ **1** and $[Pt_3\{\mu\text{-}SNC(Ph)NS\text{-}S,S'\}_2(PPh_3)_4]$ **2**. Complex **1** provides the first example of an $SNCRNS^{\bullet}$ ligand binding in a chelating manner. In the previously characterised complex[2] $[Ni_2(cp)_2\{\mu\text{-}SNC(Ph)NS\text{-}S,S'\}]$ (cp = η^5-C_5H_5) and the related[3,4] complexes $[Fe_2(CO)_6\{\mu\text{-}SNC(R)N(H)S\text{-}S,S'\}]$ the CN_2S_2 rings take up a bridging position between two metal centres, with each sulfur bonding to both metals in a μ-S, μ-S′ fashion. Complex **1** is structurally related to cisplatin $[Pt(NH_3)_2Cl_2]$ and to similar anticancer drugs[5] whilst our interest in **2** stems from its similarity to some dithiolene complexes[6] in which sulfur ligands bridge between pairs of metal ions to form one-dimensional polymers. Extensive chemistry has been carried out by Chivers, Woollins and co-workers[7] on complexes of binary sulfur–nitrogen ligands, particularly with the Group 10 metals. However, the properties[8] associated with the dithiadiazolyl radical make its co-ordination chemistry unusual and the involvement of the unpaired electron in bonding, is, in many respects, unique. We now report the detailed syntheses and full characterisation of **1** and **2** along with the first palladium dithiadiazolyl complex $[Pd_3\{\mu\text{-}SNC(Ph)NS\text{-}S,S'\}_2(PPh_3)_4]$ **3**, the palladium analogue of **2**. Their electronic properties (ESR and variable-temperature magnetic behaviour) are also reported in conjunction with an extended-Hückel molecular orbital (EHMO) study of their bonding. The biological activities of **1** and **2** are compared.

Experimental

General procedures

All reactions and manipulations were carried out using previously described procedures.[9] The NMR spectra were recorded on a Bruker AC250 spectrometer. Differential scanning calorimetry (DSC) was carried out using a Mettler FP85 thermal analyser linked to a Mettler FP80 central processor. The FAB mass spectra were obtained with a dedicated ion source fitted with a FAB atom gun. Magnetic measurements were made on a Faraday balance (Oxford Instruments) in the range 10–300 K in an applied field of 1 T. The ESR spectra were recorded on a Bruker ER200-D X-band spectrometer, UV/VIS measurements on an ATI Philips Scientific UV/VIS UV2 spectrometer, connected to an Elonex personal computer (software UV2.11).

Starting materials

The compound $(PhC\overline{NSSN})_2$ was prepared using a modification of the literature method:[9] instead of extraction of the mixed solids $[PhC\overline{NSSN}]Cl$ and LiCl by liquid SO_2 (to remove insoluble LiCl) the materials were reduced directly by Zn/Cu in tetrahydrofuran to produce a purple solution, yielding a dark solid on drying *in vacuo*. Sublimation gave crystalline $(PhC\overline{NSSN})_2$ with an increased yield [50% based on $LiN(SiMe_3)_2$]. The compounds $[Pd(PPh_3)_4]$, $[Pt(PPh_3)_4]$ and $[Pt(PPh_3)_3]$ were prepared in accordance with the literature methods.[10,11] In contrast to $(PhC\overline{NSSN})_2$, complexes **1**–**3** appear to be air-stable for several weeks. **CAUTION:** preliminary biological results (see below) show **1** to be very toxic.

Preparations

$[Pt\{SNC(Ph)NS\text{-}S,S'\}(PPh_3)_2]$·MeCN, 1·MeCN. The compound $[Pt(PPh_3)_4]$ (0.500 g, 0.402 mmol) and $(PhC\overline{NSSN})_2$ (0.073 g, 0.20 mmol) were stirred in acetonitrile (20 cm^3) to yield an immediate deep blue-green, microcrystalline precipitate in a green solution. The suspension was stirred for 20 min, the solid was then filtered off and washed with acetonitrile (3 × 10 cm^3). The pale green filtrate and washings were discarded and the microcrystalline product dried *in vacuo* (0.29 g, 76%), m.p. (from MeCN, by DSC) 136 °C (decomp.) (Found: C, 57.6; H, 3.95; N, 4.2. $C_{45}H_{38}N_3P_2PtS_2$ requires C, 57.35; H, 4.05; N, 4.45%); λ_{max}/nm (CH_2Cl_2) 680

† *Current addresses*: J. M. Rawson, Department of Chemistry, Cambridge University, Lensfield Road, Cambridge CB2 1EW, UK; A. J. Blake, Department of Chemistry, University Park, Nottingham NG7 2RD, UK.
‡ *Non-SI unit employed:* $\mu_B \approx 9.27 \times 10^{-24}$ J T^{-1}.

(ε*/dm^3 mol^{-1} cm^{-1} 1100); $\tilde{\nu}_{max}$/cm^{-1} 3051w, 1480m, 1435s (sh), 1324m, 1178w, 1160w, 1095s (sh), 1070w, 1026w, 999w, 925w, 900w, 823w, 742m, 693s, 654w (sh), 536s, 522s, 510s, 496m, 459w and 429w; ESR (X-band) $g = 2.0485$, $a_{Pt} = 5.30$, $a_P = 0.26$, $a_N = 0.55$ mT.

Crystal growth. Freshly prepared $(PhC^{\frown}NSSN^{\frown})_2$ (0.10 g, 0.28 mmol) and $[Pt(PPh_3)_3]$ (0.10 g, 0.08 mmol) were placed in separate limbs of a two-limbed vessel,[12] separated by a grade 3 glass sinter. Acetonitrile (10 cm^3) was added to each limb. After inversion of the sealed reaction vessel the $PhC^{\frown}NSSN^{\bullet}$ solution slowly diffused through the sinter and, within 30 min, dark blue-green crystals began to form over solid $[Pt(PPh_3)_3]$. After 3 d the solvent was removed yielding a number of well formed crystals suitable for X-ray analysis.

$[Pt_3\{\mu\text{-SNC(Ph)NS-}S,S'\}_2(PPh_3)_4]$ 2. The compound $[Pt(PPh_3)_4]$ (2.5 g, 2.0 mmol) and $(PhC^{\frown}NSSN^{\frown})_2$ (0.36 g, 1.0 mmol) were stirred at 80 °C in toluene (40 cm^3) to yield an immediate blue precipitate (complex **1**). After 4 h a bright orange solid was present which was filtered off, washed with fresh toluene (3 × 15 cm^3) and dried *in vacuo* (1.03 g, 85%), m.p. (DSC) broad exotherm centred at 225 °C (decomp.) (Found: C, 51.9; H, 3.5; N, 2.75. $C_{86}H_{70}N_4P_4Pt_3S_4$ requires C, 51.7; H, 3.55; N, 2.8%); $\tilde{\nu}_{max}$/cm^{-1} 3051w, 2363w, 1594w, 1571w, 1480m, 1456m, 1434s (sh), 1405w, 1303s, 1182m, 1166m, 1143m, 1095s, 1026m, 998m, 844w, 801w, 741m, 695m, 693s, 676m, 644w, 618w, 536s (sh), 523s (sh), 511s (sh), 497 (sh), 459w and 434w; δ_H(250 MHz, solvent $CDCl_3$) 7.51–7.00 (m); δ_P(250 MHz, solvent $CDCl_3$) 18.2 [*J*(PtP) 3282 Hz].

$[Pd_3\{\mu\text{-SNC(Ph)NS-}S,S'\}_2(PPh_3)_4]\cdot 2CH_2Cl_2$ 3·2CH$_2$Cl$_2$. The compound $[Pd(PPh_3)_4]$ (0.5 g, 0.43 mmol) and $(PhC^{\frown}NSSN^{\frown})_2$ (0.07 g, 0.4 mmol) were stirred in toluene (10 cm^3) for 5 h at ambient temperature. The resultant dark orange precipitate was filtered off, washed with toluene (3 × 5 cm^3) and dried *in vacuo*. Dichloromethane (5 cm^3) was added to the washed precipitate and the mixture refluxed for 10 min to yield a red microcrystalline solid under a red solution. This was cooled to room temperature, filtered and the crystalline precipitate dried *in vacuo* (0.20 g, 75%), m.p. (from CH_2Cl_2 by DSC) 270 °C (decomp.) (Found: C, 55.6; H, 3.9; N, 2.95. $C_{88}H_{78}Cl_4N_4P_4Pd_3S_4$ requires C, 55.6; H, 3.9; N, 2.95%); $\tilde{\nu}_{max}$/cm^{-1} 3051w, 1959w, 1890w, 1811w, 1594w, 1479 (sh), 1451w, 1434s (sh), 1381w, 1309s (sh), 1181w, 1168m, 1148w, 1094m, 1069w, 1026m, 998m, 920w, 902w, 845w, 822w, 739m, 714s (sh), 692s, 669s (sh), 650w, 618w, 527s (sh), 519s (sh), 506s (sh), 492m, 449w and 440w; δ_H(250 MHz, solvent $CDCl_3$) 7.34–6.94 (m) and 5.30 (s) (CH_2Cl_2); δ_P(250 MHz, solvent $CDCl_3$) 26.2 (s).

Crystal growth of complexes **2**·2C$_6$H$_5$Me *and* **3**·2CH$_2$Cl$_2$. These were carried out in an analogous manner to that for complex **1**·MeCN, except in toluene and dichloromethane respectively. Crystals suitable for diffraction studies formed within 48 and 3 h for **2** and **3** respectively.

Crystallography

The crystal data for **1**·MeCN and **2**·2C$_6$H$_5$Me have been reported previously.

Crystal data. $C_{88}H_{78}Cl_4N_4P_4Pd_3S_4$, **3**·2CH$_2Cl_2$, $M = 1904.66$, triclinic, space group $P\bar{1}$, $a = 14.242(1)$, $b = 14.261(1)$, $c = 24.512(2)$ Å, $\alpha = 73.44(1)$, $\beta = 89.19(1)$, $\gamma = 62.09(1)°$, $U = 4175$ Å^3, $\lambda = 0.710\,73$ Å, $Z = 2$, $D_c = 1.515$ g cm^{-1}, $T = 150$ K, $\mu = 0.99$ mm^{-1}.

Data collection and processing. A Siemens SMART-CCD three-circle diffractometer with an Oxford Cryosystems low-temperature device,[13] graphite-monochromated Mo-Kα X-radiation and an area detector were used. Data collection, processing and an absorption correction were carried out as described previously.[14] Indices were $-16 \leqslant h \leqslant 16$, $-14 \leqslant k \leqslant 15$, $-29 \leqslant l \leqslant 29$.

Structure solution and refinement. The structure was solved by Patterson methods using SHELXS 86[15] and refined using full-matrix least squares on F^2.[16] All elements heavier than C were refined anisotropically; H atoms were added at calculated positions. Convergence was obtained at $R1[F_o > 4\sigma(F_o)] = 0.0674$, $wR2 = 0.1686$ $\{w = 1/[\sigma^2(F_o^2) + 0.0618P^2 + 6.03P]\}$, $S = 1.017$ for 14 375 independent observed reflections [$4.04 \leqslant 2\theta \leqslant 50°$], using 524 parameters and six restraints. The largest peak/trough in a final difference synthesis was within ±1.0 e Å^{-1}.

Atomic co-ordinates, thermal parameters, and bond lengths and angles for all three structures have been deposited at the Cambridge Crystallographic Data Centre (CCDC). See Instructions for Authors, *J. Chem. Soc., Dalton Trans.*, 1997, Issue 1. Any request to the CCDC for this material should quote the full literature citation and the reference number 186/299.

Magnetic measurements

These were carried out on a high-sensitivity Faraday balance (Oxford Instruments) in the region 10–300 K using an applied field of 1 T with a sensitivity of the order of 10^{-5} cm^3. Diamagnetic corrections were applied using Pascal's constants.

Biological studies

Primary *in vitro* antitumour screen. Primary *in vitro* screening for antitumour activity was conducted against two human tumour cell lines, SW620 colon carcinoma[17a] and the SK-OV-3 ovarian carcinoma.[17b] All lines were obtained from the European Collection of Animal Cell Cultures. Details of the use of these cell lines for chemosensitivity testing are described elsewhere.[18] The SW620 cell lines was maintained in Leibovitz L15, and the SK-OV-3 cell line in Eagles Minimal Essential Medium. All media were supplemented with 10% foetal bovine serum, penicillin (100 IU cm^{-3}) and streptomycin (100 μg cm^{-3}). All media and supplements were obtained from Imperial Laboratories (Andover, Hants., UK). The compounds were dissolved in 10% dimethylacetamide (dma) in phosphate-buffered saline at a concentration of 2 mg cm^{-3}. The cells were seeded onto 96-well microtitre plates at a concentration of 5×10^4 cells cm^{-3}. After a 24 h pre-incubation period, the cells were treated with test compound for 4 h at concentrations of 0–200 μg cm^{-3}. The compound-containing medium was then replaced with fresh medium and the cells incubated for 72 h. Cell growth was assayed using sulforhodamine B.[19] Cell survival (%) was calculated relative to untreated control cells. Dose *vs.* survival curves were constructed from these data and the IC_{50} (concentration of compound giving 50% survival) calculated. The platinum-containing anticancer drug, cisplatin, was included as a reference in all tests.

Disease-orientated *in vitro* assay of antitumour activity. Six human ovarian carcinoma cell lines, HX62, SK-OV-3, CHl, CHlcisR, A2780 and A2780cisR, were used; SK-OV-3 was obtained from the American Type Culture Collection and A2780 and A2780cisR were kindly provided by Dr. T. Hamilton (Fox Chase Cancer Center, Philadelphia, PA, USA). The establishment details and platinum drug chemosensitivity properties of these lines have been described previously.[20] The cell lines CHlcisR and A2780cisR represent those derived from their respective parent lines, but which possess an acquired resistance (*ca.* 6- and 12-fold respectively) to cisplatin. The cell lines were grown as monolayer cultures in Dulbecco's Modified Eagle's Medium containing 10% foetal bovine serum (Life Technology Ltd, Paisley, UK), supplemented with gentamycin (50 μg cm^{-3}),

* The solution decomposition of complex **1** (to give **2**) hinders precise calculation of its absorption coefficient.

amphotericin (2.5 μg cm^{-3}), insulin (10 μg cm^{-3}), hydrocortisone (0.5 μg cm^{-3}) and L-glutamine (2 mmol dm^{-3}) in 6% CO_2–air atmosphere. All lines were free of mycoplasma during the course of this study. Compounds **1** and **2** were dissolved in dma (25 mg cm^{-3}) immediately before use. Growth inhibition was then assessed using a 96 h drug exposure and sulforhodamine B assay as described previously.[20] Cells were seeded at (3–5) × 10^3 cells cm^{-3} per well in 96-well microtitre plates and allowed to attach overnight before drug addition in quadruplicate wells. Following drug exposure, the remaining cells were fixed in 10% ice-cold trichloroacetic acid and quantified using 0.4% sulforhodamine B dissolved in 1% acetic acid.

Results and Discussion

The platinum complex [Pt{SNC(Ph)NS-*S*,*S*′}$(PPh_3)_2$] **1** was formed as a blue-green microcrystalline precipitate on addition of MeCN to a mixture of [$Pt(PPh_3)_3$] and $(PhC\overline{NSSN})_2$. Elemental analysis indicated that the complex was obtained as its MeCN solvate. The FAB mass spectra (positive ion) of **1** shows the parent ion [Pt{SNC(Ph)NS-*S*,*S*′}$(PPh_3)_2$]$^+$ at *m/z* 901 and its breakdown product $Pt(PPh_3)_2$ at *m/z* 719. In addition, further peaks at higher *m/z* were observed and were assigned as [Pt_2{μ-SNC(Ph)NS-*S*,*S*′}$(PPh_3)_2$]$^+$ (1620), [Pt_2{μ-SNC(Ph)NS-*S*,*S*′}$(PPh_3)_3$]$^+$ (1358) and [Pt_2{μ-SNC(Ph)NS-*S*,*S*′}$(PPh_3)_2$]$^+$ (1096). It is not uncommon for monometallic species to dimerise in the FAB source.[21] The UV/VIS spectrum of **1** in dichloromethane shows an absorbance at the red end of the visible spectrum (λ_{max} = 680 nm) which gives rise to its intense blue colour in solution. Although the concentration of solutions of **1** could not be measured accurately (because of decomposition to **2**, see below), the magnitude of the absorption coefficient (ε = *ca.* 1 × 10^3 dm^3 mol^{-1} cm^{-1}) is indicative of a metal-to-ligand charge-transfer absorption. The intensity of this band decreases with time as **1** is converted into **2**.

Structure of complex 1

Crystals of complex **1**·MeCN suitable for X-ray diffraction were grown by slow diffusion techniques. The structure of **1** (Fig. 1) shows an unusual monometallic dithiadiazolyl complex in which the metal of a $Pt(PPh_3)_2$ unit inserts into the S–S bond of the dithiadiazolyl ring forming a six-membered metalloheterocycle. This ring-opening chelation is a novel feature of dithiadiazolyl chemistry, and previously reported structures have all shown the dithiadiazolyl radical to exhibit a bridging mode between two metal ions. Roesky *et al.*[22] have previously shown that heterocyclic thiadiazoles can also undergo ring-opening chelation with Group 10 metals, with insertion of the Group 10 metal into an S–N bond. The greater size of the metal atom in **1**, compared with Ni, assists the S–S bond in the $PhC\overline{NSSN}$ ring to expand further to accommodate the metal (*cf.* $d_{S\cdots S}$ in $(PhC\overline{NSSN})_2$,[23] [$Ni_2(cp)_2${μ-SNC(Ph)NS-*S*,*S*′}][2] and **1** is 2.089(5), 2.905(2) and 3.168(4) Å respectively). The platinum centre adopts a four-co-ordinate planar geometry, with the PtP_2S_2 and CN_2S_2 planes forming an angle of 24°, due to the inevitable ring buckling that occurs to accommodate, with minimum strain, the extra metal atom in the ring.* The thiadiazole complex [Pt{NC(CN)NC(CN)S-*N*,*S*}$(PPh_3)_2$] exhibits similar planar heterocyclic and P_2NS geometries, but in this case the angle between the two planes is only 12.8°.[22] The square-planar environment about the Pt is typically associated with a 16e^- system and this can be thought to arise from the metal (10e^-), the two phosphine ligands (each 2e^- donors) and two σ-bonded sulfur atoms (each 1e^- donors). The unpaired dithiadiazolyl electron does not appear to be intimately associated with the bonding. The environment of the unpaired electron is better described in terms of molecular orbital theory (below), and the free-radical nature of **1** is highlighted by some of its physical properties.

* An ideal planar six-membered ring will possess internal angles of 120°. By forcing one angle (at Pt) to be close to 90° then the six-membered ring will buckle to alleviate this ring strain.

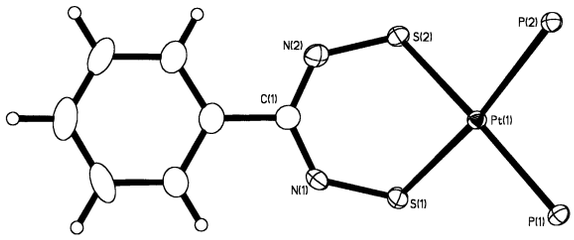

Fig. 1 Crystal structure of complex **1** (MeCN solvate and PPh_3 phenyl groups removed for clarity)

Magnetic studies on complex 1

Magnetic studies on complex **1** were carried out in the region 10–300 K using the Faraday-balance technique. The data fit the Curie–Weiss law [$\chi = C/T - \theta$)] (θ = 4 K) and the magnetic moment is typical of an $S = \frac{1}{2}$ spin-only paramagnet (1.73 μ_B). A slight rise in the magnetic moment is observed at low temperature, and this can be attributed to a small quantity of $PhC\overline{NSSN}^{\bullet}$ monomer impurity. Consistent with this hypothesis, dissolution of crystalline **1** in CH_2Cl_2 immediately gives a complex ESR spectrum, with peaks attributable to both **1** and $PhC\overline{NSSN}^{\bullet}$.

The solution ESR spectrum[1] of complex **1** could be observed, free of $PhC\overline{NSSN}^{\bullet}$ contaminant, by preparing **1** *in situ*, with an excess of [$Pt(PPh_3)_3$]. The latter reacts with $PhC\overline{NSSN}^{\bullet}$ formed through decomposition of **1** during the formation of **2** (see below). The shift in the *g* value away from that of the free electron[24] (*g* = 2.0485, *cf.* g_e = 2.0023) is consistent with delocalisation of the unpaired spin density away from the heterocyclic ring and towards the metal centre, and this is confirmed by the large hyperfine coupling to Pt, and smaller coupling to both N and P nuclei (a_{Pt} = 5.30, a_P = 0.26, a_N = 0.55 mT). The hyperfine coupling constants indicate that the unpaired electron occupies a molecular orbital which is extensively delocalised over the metalloheterocyclic framework with coupling to platinum, two nitrogen and two phosphorus nuclei (see EHMO calculations, below). Owing to the presence of this unpaired electron, the ^{1}H NMR spectrum is affected by paramagnetic broadening and is poorly resolved; the aromatic protons are greatly affected and the only sharp resonance is for the solvate molecule (MeCN) in the crystal lattice (δ_H 2.00). The sharpness of this peak is consistent with the structural data which indicate that the acetonitrile molecule is not involved in co-ordination to Pt. No peak attributable to **1** can be observed in the ^{31}P NMR spectrum between δ +300 and −300, even when the complex is prepared *in situ* from [$Pt(PPh_3)_4$] and $(PhC\overline{NSSN})_2$. This is not surprising as it is often the case that species that yield good ESR spectra usually have NMR resonances too broadened to be observable.[25]

Molecular orbital calculations

Although heavy metals such as platinum are not particularly suited to such calculations, qualitative information derived from them may prove valuable in understanding the bonding and, in this instance, the electronic properties of these complexes. The EHMO calculations were carried out on the parent complex [Pt{SNC(H)NS-*S*,*S*′}$(PH_3)_2$] using the CACAO package[26] in order to examine the nature of the frontier molecular orbitals. The geometry used was that observed in the crystallographic study but phenyl groups were replaced by protons at 1.08 Å.

Table 1 Selected bond lengths (Å) and angles (°) for complexes **1**–**3**

1		**2**		**3**	
Pt(1)–S(1)	2.294(2)	Pt(1)–S(1)	2.367(4)	Pd(1)–S(1d)	2.356(2)
Pt(1)–S(2)	2.309(2)	Pt(1)–S(2)	2.387(4)	Pd(1)–S(2d)	2.361(2)
		Pt(2)–S(1)	2.332(5)	Pd(1)–S(3d)	2.332(2)
		Pt(2)–S(2)	2.344(4)	Pd(1)–S(4d)	2.346(2)
				Pd(2)–S(3d)	2.359(2)
				Pd(2)–S(4d)	2.402(3)
Pt(1)–P(1)	2.311(2)	Pt(1)–P(2)	2.301(4)	Pd(3)–S(1d)	2.371(2)
Pt(1)–P(2)	2.322(2)	Pt(1)–P(1)	2.300(5)	Pd(3)–S(2d)	2.374(2)
				Pd(2)–P(1)	3.323(3)
				Pd(2)–P(2)	2.345(3)
				Pd(3)–P(3)	2.334(3)
				Pd(3)–P(4)	2.351(3)
		Pt(1)···Pt(2)	2.865(1)	Pd(1)···Pd(2)	2.8693(12)
				Pd(1)···Pd(3)	2.8499(11)
S(1)–N(1)	1.628(7)	S(1)–N(1)	1.66(1)	S(1d)–N(1d)	1.643(8)
S(2)–N(2)	1.648(7)	S(2)–N(2)	1.64(1)	S(2d)–N(2d)	1.648(7)
				S(3d)–N(3d)	1.631(8)
				S(4d)–N(4d)	1.649(7)
N(1)–C(1)	1.36(1)	N(1)–C(1)	1.31(2)	N(1d)–C(1d)	1.330(11)
N(2)–C(1)	1.33(1)	N(2)–C(1)	1.34(2)	N(2d)–C(1d)	1.304(11)
				N(3d)–C(2d)	1.328(11)
				N(4d)–C(2d)	1.310(11)
P(1)–Pt(1)–P(2)	100.01(7)	P(1)–Pt(1)–P(2)	103.3(2)	P(1)–Pd(2)–P(2)	102.25(10)
				P(3)–Pd(3)–P(4)	101.43(9)
P(1)–Pt(1)–S(1)	87.82(7)	P(1)–Pt(1)–S(1)	90.5(2)	P(2)–Pd(2)–S(4d)	89.83(9)
P(1)–Pt(1)–S(2)	170.21(7)	P(2)–Pt(1)–S(2)	87.8(2)	P(1)–Pd(2)–S(3d)	90.37(9)
P(2)–Pt(1)–S(1)	172.16(7)	P(1)–Pt(1)–S(2)	165.3(2)	P(1)–Pd(2)–S(4d)	163.09(9)
P(2)–Pt(1)–S(2)	85.43(7)	P(2)–Pt(1)–S(1)	166.2(2)	P(2)–Pd(2)–S(3d)	165.05(9)
				P(3)–Pd(3)–S(1d)	90.93(9)
				P(4)–Pd(3)–S(2d)	87.35(9)
				P(3)–Pd(3)–S(2d)	165.76(9)
				P(4)–Pd(3)–S(1d)	166.78(9)
S(1)–Pt(1)–S(2)	86.76(8)	S(1)–Pt(1)–S(2)	78.8(2)	S(3d)–Pd(2)–S(4d)	79.64(8)
				S(1d)–Pd(3)–S(2d)	79.62(8)
		Pt(1)–Pt(2)–Pt(1′)	180.0	Pd(3)–Pd(1)–Pd(2)	176.56(4)
		S(1)–Pt(2)–S(2)	80.4(2)	S(1d)–Pd(1)–S(2d)	80.20(8)
		S(1)–Pt(2)–S(2′)	99.6(2)	S(1d)–Pd(1)–S(3d)	174.98(10)
		S(1)–Pt(2)–S(1′)	180.0	S(1d)–Pd(1)–S(4d)	98.74(9)
		S(2)–Pt(2)–S(2′)	180.0	S(2d)–Pd(1)–S(4d)	178.00(10)
				S(3d)–Pd(1)–S(2d)	99.86(9)
				S(3d)–Pd(1)–S(4d)	81.34(8)
		Pt(2)–S(1)–Pt(1)	75.1(1)	Pd(1)–S(1d)–Pd(3)	74.15(7)
		Pt(2)–S(2)–Pt(1)	74.5(1)	Pd(1)–S(2d)–Pd(3)	74.01(7)
				Pd(1)–S(3d)–Pd(2)	75.41(7)
				Pd(1)–S(4d)–Pd(2)	74.35(7)
N(1)–S(1)–Pt(1)	115.2(2)	N(1)–S(1)–Pt(1)	111.1(5)	N(1d)–S(1d)–Pd(1)	106.5(3)
N(2)–S(2)–Pt(1)	115.1(2)	N(1)–S(1)–Pt(2)	107.4((6)	N(1d)–S(1d)–Pd(3)	112.4(3)
		N(2)–S(2)–Pt(1)	113.2(5)	N(2d)–S(2d)–Pd(1)	107.9(3)
		N(2)–S(2)–Pt(2)	109.3(5)	N(2d)–S(2d)–Pd(3)	111.4(3)
				N(3d)–S(3d)–Pd(1)	111.9(3)
				N(3d)–S(3d)–Pd(2)	105.0(3)
				N(4d)–S(4d)–Pd(1)	108.6(3)
				N(4d)–S(4d)–Pd(2)	109.1(3)

The highest fully occupied molecular orbital (HFOMO), the singly occupied molecular orbital (SOMO) and the lowest unoccupied molecular orbital (LUMO) are illustrated in Fig. 2. The first striking feature is that all three frontier orbitals are of π-type character, and that the HFOMO and SOMO of the dithiadiazolyl radical[8] are key components in the corresponding HFOMO and SOMO of complex **1**. The SOMO is formed by interaction of the platinum d_{xz} orbital with the SOMO of the $HC\overline{NSSN}^{\bullet}$ radical and is antibonding with respect to both S–N and S-Pt. As with dithiadiazolyl radical itself, the SOMO is nodal at carbon. The SOMO defines the distribution of unpaired spin density and consequently can be directly related to ESR experiments. The SOMO of **1** possesses contributions from N, S and Pt, of which both N and Pt have high-abundance non-zero spin nuclei. The observed ESR spectrum exhibits hyperfine coupling to two N and one Pt nucleus. In addition, phosphorus hyperfine interactions are also observed, despite the fact that the SOMO has no orbital contribution from phosphorus (the d_{xz} orbital on Pt does not possess the correct symmetry to interact with the phosphorus lone pair). However, if we consider d orbitals on P (which were not included in the EHMO calculation), then these do have the correct orbital symmetry to interact with Pt and the phosphorus hyperfine coupling can be considered to arise through d_{π}–d_{π} back donation from Pt to the phosphine ligand. In contrast, the SOMO of the nickel complex $[Ni_2(cp)_2\{\mu$-SNC(Ph)NS-*S*,*S*′$\}]$ is based on the Ni, S and C atoms and leads to a singlet resonance[4] because the major natural isotopes of all these elements have $I = 0$.

Decomposition of complex 1

Solutions of complex **1** in toluene, CH_2Cl_2 and tetrahydrofuran gradually lose their intense blue colour, forming an orange solu-

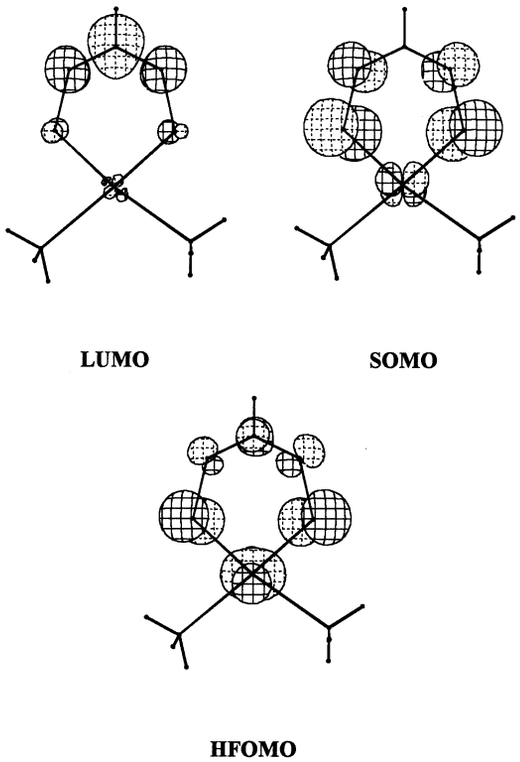

Fig. 2 Frontier molecular orbitals of [Pt{SNC(H)NS-*S*,*S*′}$(PH_3)_2$]

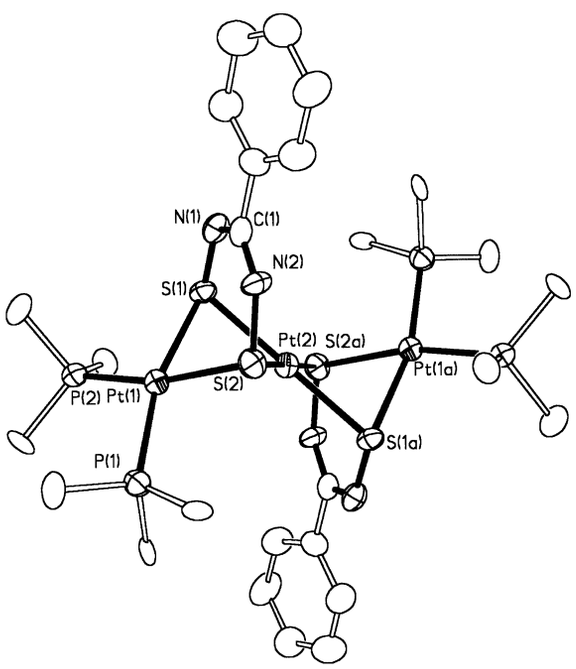

Fig. 3 Crystal structure of complex **2** (C_6H_5Me solvate molecules and PPh_3 C atoms not bonded to P removed for clarity)

tion over an orange powder; the solid was subsequently found to be the trimetallic species, [Pt_3{μ-SNC(Ph)NS-*S*,*S*′}$_2(PPh_3)_4$], **2**. As was previously stated, the ^{31}P NMR spectrum of **1** in $CDCl_3$ showed no peak that could be attributed to the monometallic complex. However, an immediate loss of PPh_3 (δ −5.1[27a]) was observed, as well as the formation of **2** [δ 18.2, J_{Pt-P} = 3282 Hz] and (over time) variable amounts of Ph_3PS (δ 43.6[27b]). A small amount of an unknown substance (δ 15.4, J_{Pt-P} = 3552 Hz) was also observed (see below). Decomposition of **1** to form **2** involves substitution of phosphine ligands by sulfur lone pairs and, for example, **2** can be thought of as being composed of a naked Pt atom, sandwiched by two molecules of **1**. A more

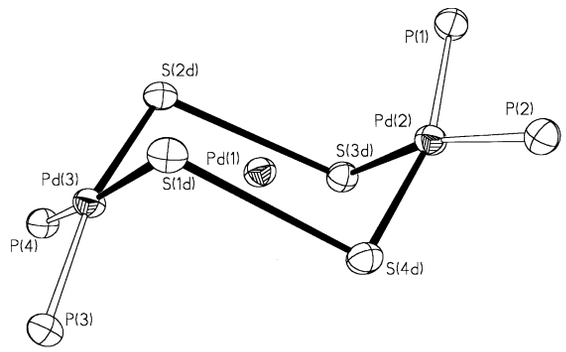

Fig. 4 The $Pd_3S_4P_2$ core in the structure of complex **3**, emphasising the chair conformation of the Pd_2S_4 ring which encapsulates a Pd atom

extensive discussion of the decomposition pathway will be described in a forthcoming publication.[28]

When the reaction was repeated in toluene a blue-green precipitate of complex **1** was formed initially which decomposed on heating to give an orange precipitate of **2**. Crystals of **2**·2C_6H_5Me, suitable for X-ray diffraction, were grown by slow diffusion techniques. In contrast, the addition of toluene to a mixture of PhC$\overline{\text{NSSN}}^{\bullet}$ and [$Pd(PPh_3)_4$] resulted only in the formation of an orange-red precipitate of [Pd_3{μ-SNC(Ph)NS-*S*,*S*′}$_2(PPh_3)_4$] **3**, analogous to **2**. Compound **3** could be recrystallised from CH_2Cl_2 as bright red diamonds. No monometallic palladium complex analogous to **1** was observed. Crystals of **3**·2CH_2Cl_2 suitable for X-ray analysis were also grown by slow diffusion methods.

Structures of complexes 2 and 3

Although complexes **2** (Fig. 3) and **3** are essentially isostructural, **2** possesses a crystallographic inversion centre whereas **3** does not. Complex **2** is composed of a linear Pt_3 chain bridged by two PhC$\overline{\text{NSSN}}$ ligands in which the terminal Pt atoms are related through a crystallographic inversion centre at Pt(2). For both **2** and **3** all the metal atoms possess planar co-ordination geometries. The terminal metals have a P_2S_2 co-ordination environment, whereas the central metal is bound only to S atoms from the heterocyclic ligand, thus producing an S_4 co-ordination geometry. As in **1**, the S–S bond is almost completely broken [for **2**, d_{SS} = 3.046(8) Å and for **3**, average d_{SS} = 3.044(8) Å], but in both **2** and **3** the dithiadiazolyl ligand takes up a bridging mode between terminal and central atoms. In **2** the Pt···Pt distance is 2.865(1) Å and in **3** the Pd···Pd distance averages 2.860(1) Å (*cf.* M···M in the nickel and related iron complexes[1–3] [$Ni_2(cp)_2$]{μ-SNC(Ph)NS-*S*,*S*′}] and [$Fe_2(CO)_6$]{μ-SNC(Ph)N(H)S-*S*,*S*′}] at 2.441(1) and 2.533(2) Å respectively). These metal–metal distances are slightly longer than the sum of the metallic radii (2.76 Å for Pt and Pd) and therefore metal–metal bonding can be considered negligible. In both **2** and **3** the core structure can be envisaged as a six-membered M_2S_4 ring in a chair conformation, with a metal atom at the centre (Fig. 4). The transannular S···S contacts between adjacent dithiadiazolyl rings [*e.g.* S(1d)···S(4d) and S(2d)···S(3d) for **3** in Fig. 4] are 3.571(8) Å for **2** and average 3.580(8) Å for **3**, somewhat longer than the distance observed in the transoid-dithiadiazolyl dimers,[29] [(*m*-NCC_6H_4)C$\overline{\text{NSSN}}$]$_2$, [(*m*-NCC_6F_4)C$\overline{\text{NSSN}}$]$_2$ and [($C_{10}H_{15}$)C$\overline{\text{NSSN}}$]$_2$ [3.141(1), 3.132 and 3.036(3) Å respectively].

Bonding in dithiadiazolyl complexes

The bonding in the nickel complex previously reported[2] can be readily described in terms of each sulfur acting as a bridging RS^- ligand, *i.e.* as a one-electron σ donor to the first metal, and a two-electron (lone-pair) donor to the second [the dithiadiazolyl

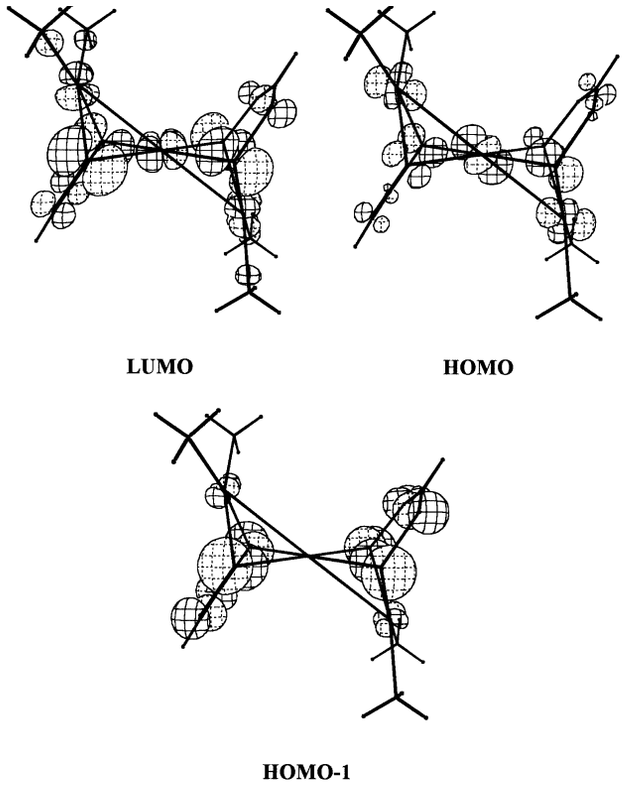

Fig. 5 Frontier molecular orbitals of $[Pt_3\{\mu\text{-SNC(H)NS-}S,S'\}_2(PH_3)_4]$

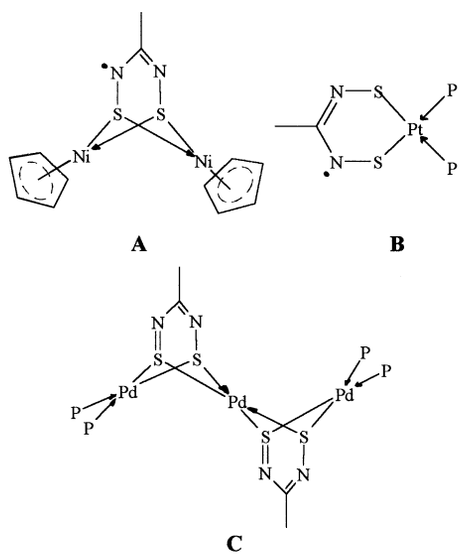

radical acts as a six-electron donor (**A**) dianion with two (cp)-Ni^+ fragments]. In the radical complex **1** only the sulfur, one-electron σ-donor electrons are used, *i.e.* the dithiadiazolyl radical chelates as a two-electron donor dianion (**B**) to one Pt^{2+} ion. This bonding mode is similar to that observed in **A**, except that the lone pairs are not involved in co-ordination in this monometallic complex. In the trimetallic complexes **2** and **3** the ligands are no longer radicals, and each heterocyclic ligand is a five-electron donor (**C**). This can be thought to arise through the formation of a N=S double bond from the unpaired electron and one of the six possible donor electrons (used in the bonding in $[Ni_2(cp)_2\{\mu\text{-SNC(Ph)NS-}S,S'\}]$).* Using this bonding approach, all three complexes (**1**–**3**) possess $16e^-$ configurations, consistent with their square-planar geometries.

The net $16e^-/16e^-/16e^-$ M_3 system and the potential for metal–metal orbital overlap (see below) between the three metal atoms would thus appear to rationalise the remarkable stability of the complex and may thus explain the absence of any polymeric materials [commonly formed as by-products in the reaction of $(PhC\overline{NSSN})_2$ with metal carbonyls[30]]. Both structures **2** and **3** are similar to linear trimetallic complexes of Pt and Pd with bridging sulfur-donor atoms ($C_6F_5S^-$).[31] However, in order to probe the complex bonding in **2** and **3** we also carried out EHMO calculations.

EHMO calculations on complex 2

The EHMO calculations on the parent analogue of complex **2**, *viz*. $[Pt_3\{\mu\text{-SNC(H)NS-}S,S'\}_2(PH_3)_4]$ were carried out using the CACAO program.[26] The frontier molecular orbitals are illustrated in Fig. 5 and indicate extensive delocalisation over the whole of the core structure. In the following discussion the metal orbitals are described in terms of their own internal geometries in which the *z* axis is perpendicular to the square plane and the *x* and *y* axes point between the ligands, with *y* in the general direction of the metal–metal vector. The structures of both **2** and **3** are similar to that reported for the nickel complex[24] $[Ni_2(cp)_2\{\mu\text{-SNC(Ph)NS-}S,S'\}]$ in that the dithiadiazolyl ring takes up a bridging mode between two metals. However, their physical properties, in comparison to the nickel complex, are markedly different; the nickel complex is paramagnetic whereas both **2** and **3** are diamagnetic. These physical differences can be rationalised through their bonding.

The LUMO of $[Pt_3\{\mu\text{-SNC(H)NS-}S,S'\}_2(PH_3)_4]$ is formed by interaction of the $HC\overline{NSSN}^{\bullet}$ SOMO with d orbitals on the metal atoms and is similar to that of the previously reported[4] nickel complex $[Ni_2(cp)_2\{\mu\text{-SNC(Ph)NS-}S,S'\}]$. In the latter case, the unpaired electron on the $HC\overline{NSSN}$ ring is transferred to a SOMO based on the Ni, S, C framework. In the case of **2** and **3** the two unpaired electrons (each derived from one of the SOMOs of the bridging dithiadiazolyl radicals) are combined to give a fully occupied molecular orbital (HOMO). Thus, although the nickel complex is paramagnetic, the platinum and palladium complexes are diamagnetic. The second highest occupied molecular orbital (HOMO−1) is analogous to the HFOMO of the nickel complex and is composed of π-based orbitals (antibonding with respect to S–S) on the dithiadiazolyl ligands; the central Pt atom is nodal with small contributions from the terminal Pt atoms.

Physical properties of complexes 2 and 3

Neither complex was found to be ESR active, in agreement with both the valence-bond and MO pictures already described. This was confirmed by Faraday-balance measurements which showed both **2** and **3** to be diamagnetic. Consequently, and in contrast to **1**, both have well resolved NMR spectra. The ^1H NMR spectra consist of aromatic proton multiplets at δ 7.51–7.00 and 7.34–6.94 respectively. The ^{31}P NMR spectra exhibit singlets, with platinum hyperfine satellites in the case of **2**, although a much weaker resonance [δ 15.4, $J_{Pt-P} = 3552$ Hz] is invariably observed in samples of **2**. The latter is attributed to a decomposition product of **2**. Its intensity increases over a period of time (days), and this is accompanied by a decrease in intensity of the initial resonance, a colour change from orange to yellow, and a simultaneous increase in the concentration of PPh_3, Ph_3PO and Ph_3PS. Samples of **3** show no such signs of decomposition. We are presently studying the redox behaviour of monometallic complexes analogous to **1** and the decomposition products derived from **2**.

* If one of the possible donor electrons is not back-donated into the heterocyclic framework, then the complex would have unpaired electrons on the sulfur–nitrogen ligand rendering the complex paramagnetic.

Table 2 Cytotoxicity of compounds **1** and **2** against two human tumour cell lines and further biological test results for **1** against a series of ovarian tumour cell lines. Results are reported as IC_{50} values *vs.* cell culture

Cell culture	**1**	**2**	cisplatin
SW620	6.3	125	120
SK-OV-3	26	110	15
A2780	0.5		8.90
A2780cisR	0.35		29.0
A2780 RF	0.7		3.3
CHl	0.43		0.082
CHlcisR	0.43		0.33
CHl RF	1		4.0
41M	0.66		0.22
41M cisR	0.7		1.05
41M RF	1.1		4.7
HX62	1.05		2.80

RF = Resistance factor = IC_{50} of resistant (cisR) line divided by IC_{50} of sensitive line.

Biological studies on complexes 1 and 2

Since the discovery of the anticancer properties of cisplatin, square-planar platinum(II) complexes have been extensively studied as potential anticancer agents.[5] The radical **1** contains a square-planar co-ordination environment about Pt and in addition also contains a free radical in close proximity to the active metal site. The close proximity of a potentially biologically active free radical to a square-planar platinum suggested that **1** may exhibit enhanced activity compared with cisplatin. In contrast, although **2** and **3** both contain square-planar metal environments, the unpaired electrons on the heterocyclic rings have become involved in bonding, and render these complexes diamagnetic.

Complexes **1** and **2** were initially tested against two human tumour cell lines (SW620 and SK-OV-3) with different sensitivities to cisplatin; the results are shown in Table 2. The values for the parent anticancer drug cisplatin are also shown for comparison. The results show that the monometallic complex, **1**, is significantly more potent than cisplatin against the SW620 colon cell line, but has a similar potency to cisplatin for the SK-OV-3 ovarian cell line. In contrast, the trimetallic complex **2** is markedly less potent than **1** and does not exhibit differential cytotoxicity towards either cell line.

Complex **1** was further tested in a disease-oriented screen consisting of a panel of human ovarian tumour cell lines and the results* are shown in Table 2. The cisR samples are cultures which have previously been exposed to cisplatin and have thus gained a degree of resistance. The resistance factor (R.F.) gives a measure of how active a complex is against a resistant strain of a culture as compared with the non-resistant strain. It is evident that **1** is more potent than cisplatin against almost all the cell strains tested. This is almost certainly mainly due to the presence of the free radical on the complex (although the presence of toxic MeCN in the lattice may also be a factor). Although these results might be deemed to be encouraging, closer examination finds that **1** exhibits very poor selectivity, *i.e.* it is very toxic towards all cell cultures. In addition, although **1** is remarkably stable to water it is also very insoluble in aqueous systems (*e.g.* the human body). Consequently, no further testing was carried out on it. However, we might expect that both the toxicities and solubilities of other derivatives may be modified through changes in both the heterocyclic radical and phosphine functional groups. Nevertheless, **1** and its derivatives should be treated with considerable care.

* The parameter employed, IC_{50}, is the concentration of compound (mg cm^{-3}) required to give a 50% decrease in cell proliferation of a culture.

Conclusion

Oxidation of zerovalent platinum and palladium phosphine complexes with $(PhC\overline{NSSN})_2$ occurs in high yield, forming both mono- and tri-metallic complexes in the case of platinum and a trimetallic complex in the case of palladium. The properties of these materials both in solution and the solid state have been examined using both physical and theoretical techniques. New bonding modes of the $PhC\overline{NSSN}$ ligand have been established, in which it can act as a chelating two- or bridging five-electron donor, highlighting the unusual nature of this ring system. We have shown that the monometallic complex **1** decomposes to give trimetallic **2** and NMR studies on **2** indicate that this slowly undergoes further decomposition. Biological tests on the monometallic complex indicate it to be extremely toxic, and it should be handled with considerable care.

Acknowledgements

We thank the EPSRC for the provision of a diffractometer (J. A. K. H.) and for three studentships (S. E. L., C. I. G. and I. M.), the EEC for a studentship (I. B. G.), Johnson Matthey plc for providing samples of $K_2[PtCl_4]$ and $PdCl_2$, G. R. Henderson (Johnson Matthey Technology Centre) for technical assistance with antitumour testing, Dr. L. Kelland (Institute of Cancer Research) for some biological antitumour testing, and the mass spectroscopy service at UMIST for FAB mass spectra.

References

1 A. J. Banister, I. B. Gorrell, S. E. Lawrence, C. W. Lehman, I. May, G. Tate, A. J. Blake and J. M. Rawson, *J. Chem. Soc., Chem. Commun.*, 1994, 1779.
2 A. J. Banister, I. B. Gorrell, W. Clegg and K. A. Jørgensen, *J. Chem. Soc., Dalton Trans.*, 1991, 1105.
3 A. J. Banister, I. B. Gorrell, W. Clegg and K. A. Jørgensen, *J. Chem. Soc., Dalton Trans.*, 1989, 2229.
4 R. T. Boeré, K. H. Moock, V. Klassen, J. Weaver, D. Lentz and H. Michael-Schulz, *Can. J. Chem.*, 1995, **23**, 1444.
5 J. Reedijk, *Chem. Commun.*, 1996, 801.
6 J. S. Miller and A. J. Epstein, *Prog. Inorg. Chem.*, 1976, **20**, 1.
7 T. Chivers and F. Edelmann, *Polyhedron*, 1986, **5**, 1661; P. F. Kelly, A. M. Z. Slawin, D. J. Williams and J. D. Woollins, *Chem. Soc. Rev.*, 1992, 245.
8 J. M. Rawson, A. J. Banister and I. Lavender, *Adv. Heterocycl. Chem.*, 1995, **62**, 137.
9 C. M. Aherne, A. J. Banister, I. B. Gorrell, M. I. Hansford, Z. V. Hauptman, A. W. Luke and J. M. Rawson, *J. Chem. Soc., Dalton Trans.*, 1993, 967.
10 T. Ukai, H. Kawazua and Y. Ishii, *J. Organomet. Chem.*, 1974, **65**, 253.
11 R. Ugo, F. Cariati and G. La Monica, *Inorg. Synth.*, 1989, **28**, 123.
12 A. J. Banister, M. I. Hansford, Z. V. Hauptman, A. W. Luke, S. T. Wait, W. Clegg and K. A. Jørgensen, *J. Chem. Soc., Dalton Trans.*, 1990, 2793.
13 J. Cosier and A. M. Glazer, *J. Appl. Crystallogr.*, 1986, **19**, 105.
14 J. A. K. Howard, I. Lavender, J. M. Rawson and E. A. Swain, *Main Group Chem.*, 1996, **1**, 317.
15 G. M. Sheldrick, *Acta Crystallogr., Sect. A*, 1990, **46**, 467.
16 G. M. Sheldrick, SHELXL 93, University of Göttingen, 1993.
17 (*a*) A. Leibovitz, J. C. Stinson, W. B. McCombs III, C. E. McCoy, K. C. Mazur and N. D. Mabry, *Cancer Res.*, 1976, **36**, 4562; (*b*) J. Fogh, W. C. Wright and J. D. Loveless, *J. Natl. Cancer Inst.*, 1977, **58**, 209.
18 S. P. Fricker, in *Metal Ions in Biology and Medicine*, eds. P. Collery, L. A. Poirier, M. Manfait and J. C. Etienne, John Libbey Eurotext, Paris, 1990, pp. 452–456.
19 J. D. Higgins III, L. Neely and S. P. Fricker, *J. Inorg. Biochem.*, 1993, **49**, 149.
20 L. R. Kelland, G. Abel, M. J. McKeage, M. Jones, P. M. Goddard, M. Valenti, B. A. Murrer and K. R. Harrap, *Cancer Res.*, 1993, **53**, 2581.
21 R. Davis, I. F. Groves, J. L. A. Durrant, P. Brooks and I. Lewis, *J. Organomet. Chem.*, 1983, **241**, C27.

22 H. W. Roesky, H. Hofmann, P. G. Jones and G. M. Sheldrick, *Angew. Chem., Int. Ed. Engl.*, 1984, **23**, 971.
23 A. Vegas, A. Pérez-Salazar, A. J. Banister and R. G. Hey, *J. Chem. Soc., Dalton Trans.*, 1980, 1812.
24 C. P. Poole, *Electron Spin Resonance: A Comprehensive Treatise on Experimental Technique*, 2nd edn., Wiley-Interscience, New York, 1983.
25 E. A. Ebsworth, D. W. H. Rankin and S. Cradock, *Structural Methods in Inorganic Chemistry*, Blackwell Scientific Publications, Oxford, 1987, p. 93.
26 C. Mealli and D. M. Proserpio, *J. Chem. Educ.*, 1990, **67**, 399 (PC Version 4.0, 1994).
27 V. Mark and J. R. Van Wazer, *Topics in Phosphorus Chemistry*, **5**, *^{31}P Nuclear Magnetic Resonance*, Wiley, New York, 1967, (*a*) p. 250, (*b*) p. 363.
28 A. J. Banister, C. I. Gregory, J. A. K. Howard, S. E. Lawrence, I. May, J. M. Rawson and B. K. Tanner, unpublished work.
29 A. W. Cordes, R. C. Haddon, R. G. Hicks, R. T. Oakley and T. T. M. Palstra, *Inorg. Chem.* 1992, **31**, 1802; C. M. Aherne, A. J. Banister, A. Batsanov, N. Bricklebank, W. Clegg, M. R. J. Elsegood, J. A. K. Howard, I. Lavender, S. E. Lawrence and J. M. Rawson, unpublished work; J. N. Bridson, S. B. Copp, M. J. Schriver, S. Zhu and M. J. Zaworotko, *Can. J. Chem.*, 1994, **72**, 1143.
30 I. B. Gorrell, Ph.D. Thesis, University of Durham, 1989.
31 R. Uson, J. Fornies, M. Tomas, B. Menjon, J. Carnicer and A. J. Welch, *J. Chem. Soc., Dalton Trans*, 1990, 151; R. Uson, J. Fornies, M. A. Uson, M. Tomas and M. A. Ibanez, *J. Chem. Soc., Dalton Trans.*, 1994, 401.

Received 27*th September* 1996*; Paper* 6*/*06635*F*